31st March 2021

Final Report

Research period: 31th July 2020 to 31st March 2021

Title:

"Searching the Approaches for Lithium-Ion Battery (LIB)

Second Life Performance Improvement"

"FM Lab" Co Ltd

Daniil Itkis

Summary

Title

  Searching the Approaches for Lithium-ion Battery (LIB) Second Life Performance Improvement

Research period

  31th July 2020 to 31st March 2021

Development / Survey Representative

  "FM Lab"Co Ltd   Dr. Daniil Itkis

Conductor

  "FM Lab"Co Ltd   Dr. Daniil Itkis

  Nissan Motor Co., Ltd.   Kazuyuki Shiratori

                        Yoshiko Hisitani

                        Takako Toda

Subcontractor

  "SC-Tek" LLC   Dr. Mikhail Kondratenko

<u>Purpose</u>

The main aim of the project is to monitor and to evaluate promising approaches, which can enable enhancement of the LIB performance during its second life (i.e. approaches enabling recovery of battery capacity and/or power after it was used for some time and has been degraded).

<u>Project Tasks</u>

Task 1. Verification of recovery with the original method using laminated (pouch) cells:

      1.1 Further screening of lithium salts – solubility and oxidation potentials

      1.2 Ageing of pouch cells

      1.3 Washing/refilling of cycled cells

Task 2. Design of a dedicated cell structure capable for capacity recovery by the original method, even in a non-dry environment:

      2.1 Developing the cell concept

      2.2 Cell design & sketching

      2.3 Parts fabrication & cell assembly

      2.4 Cell testing

Task 3. Drafting the conceptual design of a high-pressure rig for laminated (pouch) cell regeneration using supercritical fluids without dry environment

Task 4. Final report preparation

<u>Summary</u>

Testing of the suggested recovery approach on pouch cells revealed significant inaccuracy caused by non-optimized experimental conditions. Opening, washing, and refiling the cells with ordinary electrolyte leads to increased degradation rate and significant scatter in the cycling data. It makes hard to accurately check the effect of washing/recovery electrolyte refilling.

Although pouch cell washing by supercritical fluid and refilling with recovery electrolyte candidates did not result in capacity improvement, refilling with Li lactate-containg electrolyte significantly slowed down the degradation giving a hope of recovery possibility if experimental conditions are improved.

We suggested, designed, and tested a dedicated electrochemical cell (high-pressure electrochemical cell, HPEC), which we believe can enable more accurate experimental conditions for testing our recovery approach. The cell operation was demonstrated.

Further research should be done with longer and more standardized cell ageing to avoid unpredictable results. Pouch cell opening and resealing protocols are to be optimized.

Abbreviations

BPR	back-pressure regulator
CC	constant current
CV	constant voltage
CVA	cyclic voltammetry
DMC	dimethyl carbonate
EC	ethylene carbonate
EIS	electrochemical impedance spectroscopy
HPEC	high-pressure electrochemical cell
ICP MS	inductively coupled plasma mass spectroscopy
LAM	loss of active materials
LFP	lithium iron phosphate $LiFePO_4$
LIB	lithium-ion battery
LLI	loss of lithium inventory
LMO	lithium manganese oxide $LiMn_2O_4$
MeCN	acetonitrile
NMC	lithium-nickel-manganese-cobalt oxide $Li(Ni, Mn, Co)O_2$
NMP	N-methyl-2-pyrrolidone
PEEK	polyetheretherketone
PVDF	polyvinylidene difluoride
$scCO_2$	supercritical carbon dioxide
SCF	supercritical fluid
SEI	solid-electrolyte interphase
SEM	scanning electron microscopy
TBAP	tetrabutylammonium perchlorate

Contents

Introduction

The demands for LIBs continue to grow, one of the main drivers today is the production of electric vehicles, which have high energy efficiency (ca. 80% or higher vs. 12-30% for cars with internal combustion engines) [1]. According to various estimates [2,3], the annual amount of LIB waste is *ca.* 200-500 million tons, of which 5-15 wt. % belong to cobalt - an expensive and toxic element, and 2–7 wt.% - to lithium. Due to expected acceleration of LIB production growth the battery recycling [2–6] and "second life" [7] became quite hot topics driven by both economic and environmental factors. Although battery recycling is rather cost- and labour-consuming, increasing amount of spent batteries pushes active investments into this field. Reusing spent batteries in the applications not requiring high performance – battery "second life" – is on the contrary much less expensive. However, there are serious limitations on energy and power of the spent batteries, so the number of applications is quite limited. Economic benefits of using the spent batteries as is after EoL are also not obvious due to deteriorated performance [7].

This project aims to improve the performance of the spent lithium-ion batteries, to make it possible to use recovered ones during its "second life" in demanding applications such as electric vehicles. Although recovery of initial properties of the as-produced battery seems to be impossible, we are searching the approaches for partial restoring battery capacity and/or power. The focus of the project is evaluating the approach, which was suggested at the previous stages for enhancement of the LIB performance during its second life.

Among the numerous reasons for the battery performance loss [8] the group identified as loss of lithium inventory was suggested by us as the most important. During recent years this hypothesis was confirmed for batteries used in EVs [9] and in grid-storage applications [10]. It was also found to be true for various cathode chemistries including NMC, LMO, and LFP. The LLI is driven mainly by damaging of initial SEI layer and its re-formation leading to Li^+ capture in the form of as Li_2O, LiF, Li_2CO_3 and possibly other products. Thus, lithium is partially immobilised in SEI, thus the number of active charge carriers in the cell decreases and the capacity fades. As well, excessive SEI increases the negative electrode resistance thus lowering the cell power characteristics.

The main idea for restoring the spent battery capacity is based primarily on removing the old electrolyte and partially SEI layer from the surface of the negative electrode and further "refilling" of lithium inventory in the cell. This is illustrated in Figure 1, which shows

partial immobilization of lithium ions in SEI during battery life, removal of old SEI, refilling the lithium inventory using special "recovery" electrolytes and reformation of SEI (lithium oxalate additive to prepare "recovery" electrolyte is shown as an example).
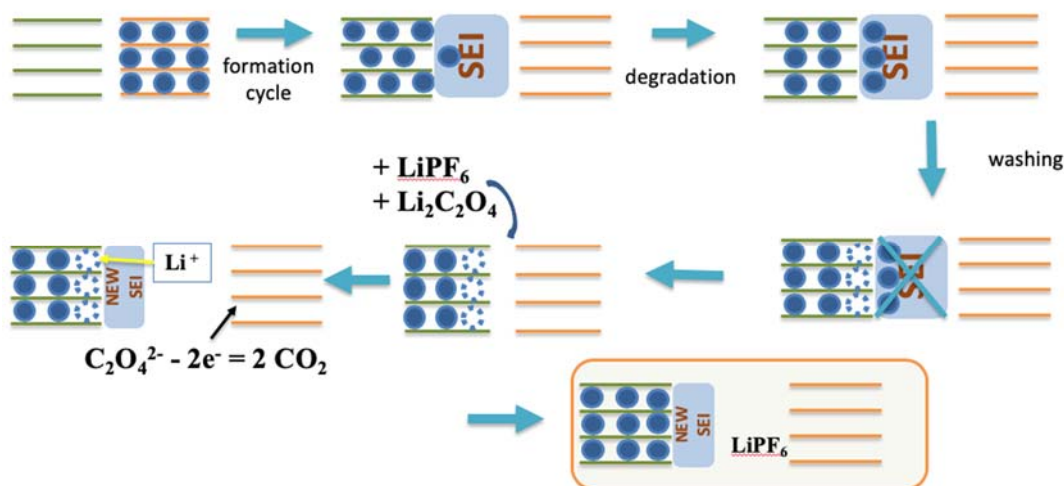

Figure 1. Schematic illustration of the project general idea. Lithium host materials are shown as green (anode) and orange (cathode) layers. Dark blue circles are lithium ions. Dotted circumflexes denote potential host sites for lithium, which are not filled.

Although complete removal of SEI depicted in Figure 1 was not yet confirmed, we previously demonstrated the ability of extracting the old electrolyte and from the electrodes using supercritical fluids, which have good permeation ability (see the reports for FY 2018 and 2019). During this project stage we further investigated removal of electrolyte from the commercial pouch cells by supercritical fluids (sc-CO_2 with MeCN as a co-solvent). The experimental setup build previously was found to be able to wash out the electrolyte from pouch cells, which was controlled by ICP MS and by measuring the cell impedance (high impedance of the washed cell evidences for the electrolyte removal). The candidates for recovery electrolyte suggested before (Li oxalate, Li acetate) were found to be poorly soluble in 1M $LiPF_6$ in EC:DMC electrolyte and can be hardly employed for lithium inventory recovery. Because of that we continued the search for the compounds, which can enable lithium inventory refilling. High-pressure electrochemical cell for cycling model lithium-ion battery was developed. It enables the internal cell volume washing and electrolyte refilling without the need for cell disassembly in argon-filled glove-box environment. The cell was tested by cycling with graphite vs. NMC electrodes, washing the electrolyte and refilling. The general concept on upgrading the designed cell into a system for real battery recovery was drafted.

Verification of the pouch cells recovery

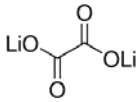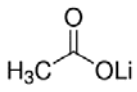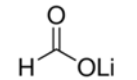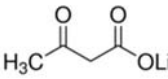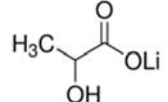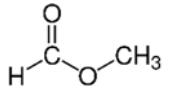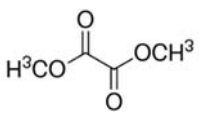## Screening of the salts for recovery electrolyte

As state above, repeated SEI formation leads to active lithium inventory loss, thus, the stated red/ox balance between cathode and anode materials becomes disrupted (see Figure 1). For balancing red/ox processes and recovering lithium inventory we tried several additions to electrolyte listed in Table 1. While selecting additives for the tests, we used two criteria: 1) the additive hypothetically can be oxidized irreversibly at moderate potentials with gaseous products formation; 2) it should provide Li^+ for lithium inventory recovery.

We monitored the lithium salts with well-known oxidizable anions: oxalate and formate. Also, acetate and nitrate, according to the literature, can be oxidized at the potentials close to electrolyte oxidative stability boundary. Acetoacetate and lactate can be converted in CO_2 and H_2O in living cells and be easily oxidized. However, solubility of organic salts in organic carbonates (EC:DMC 1:1 v/v) was found to be very low. As aprotic polar solvents, carbonates are unable to solvate anions, and solubility decreases with an increasing anion charge density (i.e., relation between anion charge and its size).

For testing the electrochemical behavior of the additives, we used 3-electrode analytical glass cell with glassy carbon (GC) as a working electrode, Pt wire as a counter electrode, polypyrrol on Pt wire (PPy^+/PPy) as a reference electrode. After each experiment the reference electrode was calibrated by measuring the ferrocene/ferrocene$^+$ redox couple potential. The EC:DMC mixture (1:1 by vol.) was used as a solvent, 0.1 M TBAP was dissolved and played a role of supporting electrolyte. Concentration of tested compounds varied from 0.05 to 0.1 M. Cycling voltammetry studies were done with a sweep rate of 50 mV/s inside the electrolyte stability window. Acetate and oxalate were tested previously (see the report for FY 2019). All results voltammograms are presented in Figure 2.

As all of the tested lithium salts were found to be either poorly soluble or demonstrated very little redox activity in these model experiments, we suggested a new approach: using lithium-free methyl formate and dimethyl oxalate as additives. Despite lithium absence, side reactions with an excess of $LiPF_6$ can possibly produce Li^+ for lithium inventory recovery. These compounds were found to be nicely soluble in EC:DMC and can be easily oxidized. However, the possibility to use them for recovery of full lithium-ion cells needs further testing.

Table 1 Selected compounds for candidate recovery electrolytes.

Name	Formula	Achievements	Problems
Lithium oxalate	LiO–C(=O)–C(=O)–OLi	- Oxidation onset between 3.5-4.0 V vs. Li$^+$/Li - Compensates lithium inventory losses in solid form being added to cathode material	Very low solubility: exact solubility value was not measured, but very high impedance of the saturated solution in EC:DMC (without LiPF$_6$) is an indirect evidence
Lithium acetate	H$_3$C–C(=O)–OLi	- Oxidation onset between 3.4-4.0 V vs. Li$^+$/Li	Very low solubility: exact solubility value was not measured, but very high impedance of the saturated solution in EC:DMC (without LiPF$_6$) is an indirect evidence
Lithium nitrate	LiNO$_3$	- Solubility in EC:DMC is at least 0.05 M	- Oxidation onset close to 4 V vs. Li$^+$/Li, higher than for other salts - Evolution of nitrogen oxides (environmental impact)
Lithium formate	H–C(=O)–OLi	- Solubility at least 0.05 M in EC:DMC	- High hygroscopicity; only hydrate is commercially available, necessity to dry
Lithium acetoacetate	H$_3$C–C(=O)–CH$_2$–C(=O)–OLi	- Oxidation onset at low potentials (starting at ca. 3.1 – 3.2 V vs. Li$^+$/Li)	- Low chemical and thermal stability - Tendency to form sol instead of true solution
Lithium lactate	H$_3$C–CH(OH)–C(=O)–OLi		- No visible oxidation activity up to 4.5 V vs. Li$^+$/Li - Solubility not higher than 0.01 M
Methyl formate*	H–C(=O)–O–CH$_3$	- Liquid, solubility in EC:DMC is at least 0.1 M	- Stable oxidation peak at 4.7 V vs. Li$^+$/Li (should be double checked)
Dimethyl oxalate*	H$_3$CO–C(=O)–C(=O)–OCH$_3$	- Solubility in EC:DMC is at least 0.1 M - Oxidation onset between 3.7-4.5 V vs. Li$^+$/Li	- Reduction onset at 2-2.4 V vs. Li$^+$/Li

* require addition of extra concentration of LiPF$_6$ for lithium inventory refilling; charge compensation is expected to be provided by interaction of residual PF$_6^-$ anions with the oxidation products.
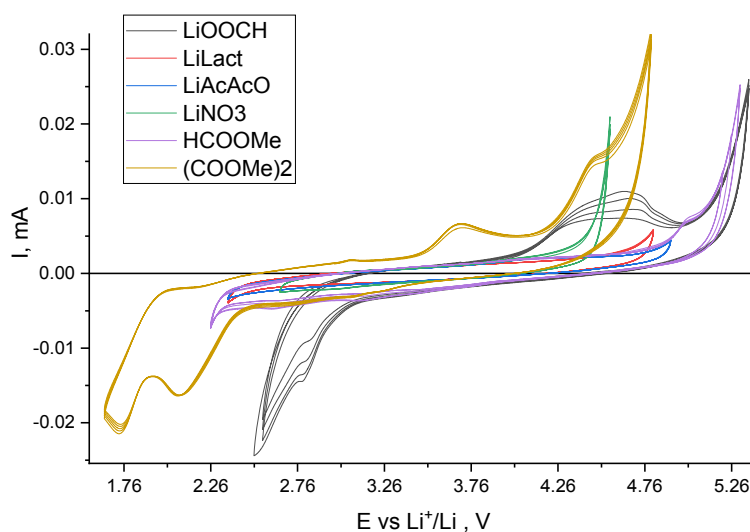
Figure 2. CVA curves for tested candidates for recovery electrolyte. Lithium formate (LiOOCH), lactate (LiLact), acetoacetate (LiAcAcO), nitrate (LiNO$_3$), methyl formate (HCOOMe), and dimethyl oxalate ((COOMe)$_2$) in EC:DMC with 0.1 M TBAP as a supporting electrolyte. The voltage sweep rate 50 mV/s.

Ageing of the pouch cells

For testing the approach on commercially produced pouch cells we selected available batteries with geometric dimensions allowing the washing in the experimental setup built during previous project stage.

Figure 3. Photograph of the pouch cell used for cycling

The used cells were produced by EEMB ltd. (model LP401730). The picture of the cell is shown in Figure 3. The cells comprise graphite – NMC chemistry. Its properties are summarized in Table 2.

Parameter	Value
Dimensions	30 mm × 17 mm × 4 mm
Nominal capacity	150 mAh at C/5
Internal resistance	< 300 mOhms
Recommended upper cutoff voltage	4.2 V
Recommended lower cutoff voltage	2.75 V
Average measured initial charge capacity	157.3 ± 2.6 mAh at C/2
Average measured initial discharge capacity	156.9 ± 2.7 mAh at C/2

The cells ageing was performed at a room temperature (23 ± 2°C) using multichannel Biologic SAS MPG2 potentiostats. Discharge was performed at 75 mA (C/2) down to 2.75 V potential. Charge was performed at CC/CV regime. Current was kept at 75 mA until the voltage reached the upper voltage threshold, which varied from one batch of the cells to another (4.20, 4.30, 4.35, and 4.40 V). Then the cell was kept at constant voltage until the current went down to 7.5 mA (10-fold decrease).
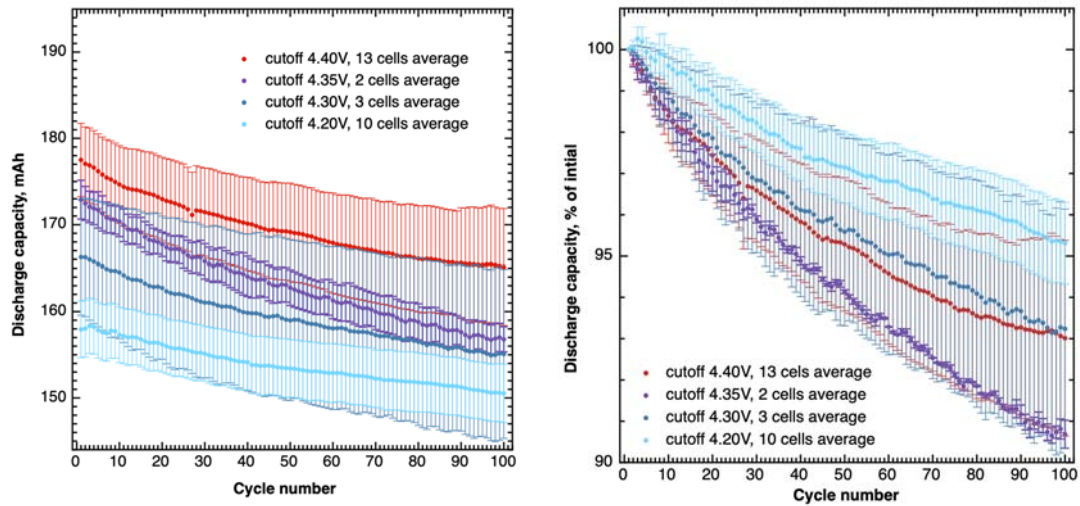

Figure 4 Average capacity fade for the pouch cells during cycling with different upper cut-off voltage (indicated in the legends). Left graph shows absolute capacity values, right – the value normalized by the first cycle. Points show mean values, error bars indicate standard deviations among the cells tested with certain upper voltage limit.

Figure 4 shows the averaged capacity fade for the aged cells. As expected, overcharging

the cells to higher voltage resulted in higher initial capacities. At the same time, the degradation rate increased enabling to reach higher capacity loss in the limited timeframe. The cells charged up to 4.35V during ageing demonstrated unexpected behaviour degrading faster than those with stronger overcharge (4.40V). While this particular case can be connected with insufficient statistics (only two cells were aged by discharge/charge to 4.35V), it should be noticed that the overcharge conditions can affect the contributions of different degradation mechanisms to capacity loss. One can imagine, as an example, the intensified Ni dissolution from the cathode material at high voltages leading to increased contribution of LAM degradation mode. Being constrained by the timeframe, however, we used the cells aged at different conditions for washing/refilling experiments. Nevertheless, the consequences of various ageing regimes, as well as other ageing approaches are to be thoroughly analysed in future.

The cells cycled with an overcharge were finally discharged/charge 10 times with 4.20V upper voltage limit to enable the comparison of the capacity drop between the cells aged in different conditions.

Supercritical washing of the pouch cells

The experiments were carried out using the setup proposed at the previous stage of the project (Figure 5). CO_2 pressure was set to 300 bar, thermostat exposition temperature = 60 °C, fluid flow 4 ml/min.

1 – CO_2 cylinder
2 – pressure generator
3 – reactor I
4 – reactor II
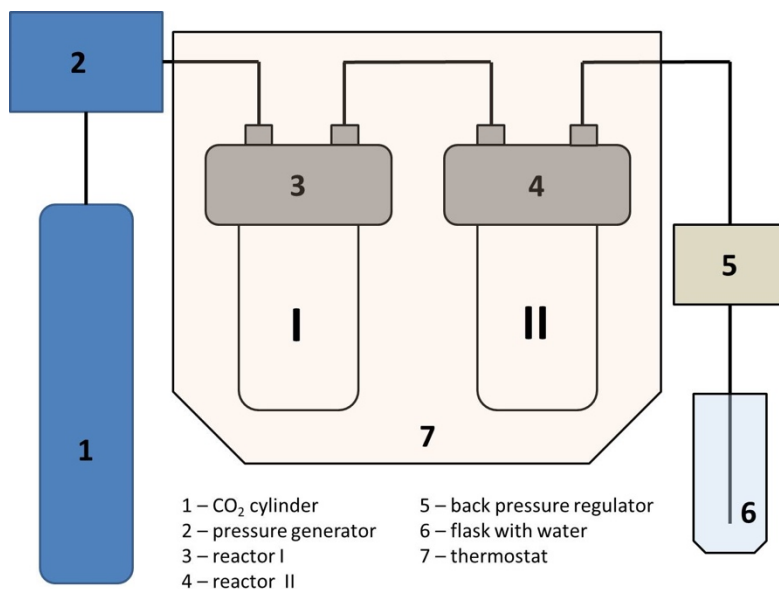5 – back pressure regulator
6 – flask with water
7 – thermostat

Figure 5. Supercritical fluid extraction setup scheme.

Each washing experiment consisted of three steps: 1) preliminary washing of the system

with deionized water, 2) washing the pouch cell with supercritical carbon dioxide with a co-solvent, 3) final washing of the system (cell removed) with water. A detailed description of each stage is given in the report for FY 2019.

We used the developed washing method for commercial pouch cells. For washing the aged cells were cut by knife on the one side and placed into the reactor II, this operation was done inside an argon-filled glove box. The reactor was sealed and isolated by the valves and connected to the high-pressure system. 50 ml of co-solvent (acetonitrile) was poured in the reactor I; the entire experimental setup was purged with CO_2 for 90 minutes, and as a result CO_2 was fed into reactor I, mixed with co-solvent, got into reactor II, mixed with electrolyte in the pouch cell and got into the flask with water. Analysing the ICP MS data, we plotted the curves showing the concentration of washed lithium versus the volume of CO_2 flushed through the system. Additionally, the procedures of pre-washing and post-washing of the reactor with water were carried out, ensuring the control of the purity of the capillaries of the setup. The lithium concentration in the post-washings was more than a hundred times lower than in the main washing procedure (CO_2 + co-solvent), which indicates that the minimum amount of lithium accumulated in the capillaries.

Figure 6 shows a typical graph of lithium extraction from the pouch cell. The data are presented as a cumulative total. The amount of Li washed from the pouch cell reaches the saturation level.
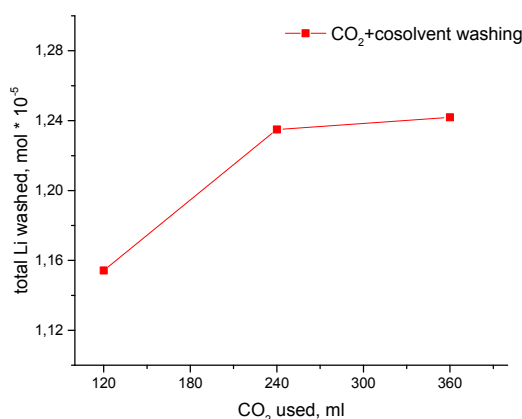

Figure 6. The amount of lithium leached from the pouch cell vs. the amount of CO_2 flushed though the cell. The plot shows typical example for washing one of the aged cells. The amount of Li was detected by means of ICP-MS analysis. MeCN used as a co-solvent.

Based on the experimental data obtained for 13 aged pouch cells, the median amount

of leached lithium was $1.5*10^{-5}$ mol. Thus, the possibility of supercritical extraction of lithium from commercial pouch cells was demonstrated.

Refilling the pouch cells

After washing by SCF the aged pouch cells were transferred back to the glove box without the contact to environment for refilling. The high-pressure reactor was flushed by pure argon prior to opening inside the glovebox to avoid contamination of the inert atmosphere by CO_2. For refilling the electrolyte solutions (ordinary electrolyte 1 M $LiPF_6$ in EC:DMC from Sigma Aldrich, or the recovery electrolyte candidates – lithium nitrate, acetoacetate or lactate dissolved in ordinary electrolyte solution) were poured inside the cell through the cut in the laminate using a pipette with a plastic tip. The refilling volume was ca. 1 ml. After refilling the cells were "resealed" by applying self-adhesive polyimide tape as the used pouch cells had not enough space for thermal welding of the cut. As it was found that the cell cutting and resealing affect the electrochemical performance (see below), part of the cells was additionally wound by laminate (on top of polyimide tape) and compressed with plastic straps (see Figure 7) to simulate external pressure on the cell lost due to cutting the body. As such a temporary "resealing" procedure cannot guarantee the airtightness, the cells after resealing were placed in vacuum-tight containers with electric feedthroughs for electrochemical testing. Only after that the "resealed" cells in the containers were taken out from the glove box. The testing after refilling was done in the 2.75 – 4.20V range, CC discharge and CC/CV recharge mode was used, 75 mA current was applied, 10-fold current drop was used as the end-of-charge criterion.
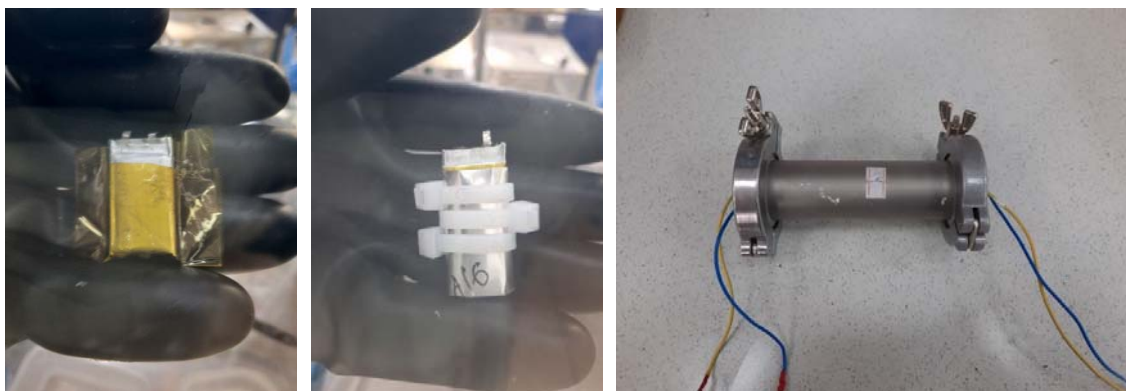

Figure 7 Pictures of the pouch cell, resealed by self-adhesive polyimide tape, similar cell additionally wound by Al-laminate and compressed by plastic straps, vacuum-tight container with electric feedthroughs for cell testing.

Before refilling the cells with recovery electrolyte candidates, we performed control experiments. First, the cells were refilled by ordinary electrolyte (1M $LiPF_6$ in EC:DMC)

after washing. Second, ordinary electrolyte was poured into the cell without washing by SCF (just opening the cell, pouring additional electrolyte, sealing by tape). The results are summarized in Figure 8. Control experiments revealed that fast degradation occur after opening/"resealing" the used type of pouch cells. At the same time data is much scattered. Now we see two main reasons for this. First, it can relate to the loss of compression between electrodes, as the cell is resealed without evacuation, thus there is no pressure difference enabling the compression of a jelly roll inside. Second, possible contamination with humidity due to impropper MeCN quality (co-solvent in supercritical washing). Both reasons to be further checked. Trials of applying additional external compression to the cell were already performed for the batteries refilled with lithium lactate and acetoacetate (see below). Monitoring of the MeCN purity and humidity to be performed.
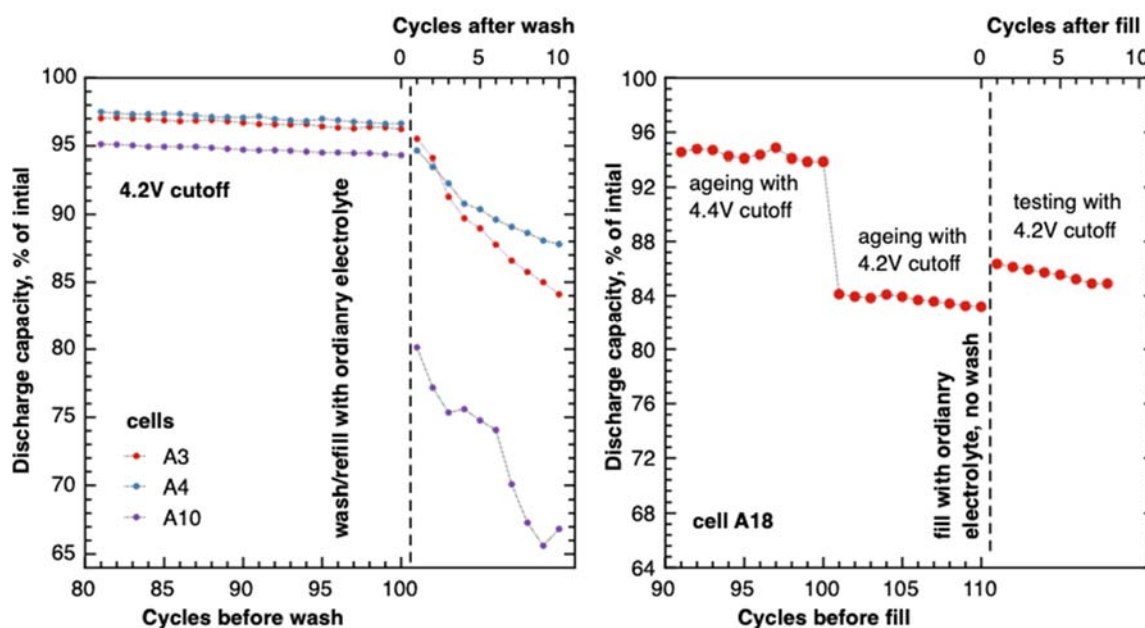

Figure 8. (Left) relative capacity fade (normalized by the first cycle of a certain cell) before and after opening the cell, washing by SCF, refiling with ordinary electrolyte, and resealing by polyimide tape (without external compression of the cell). Three pouch cells were aged in the same conditions with 4.2V upper voltage cutoff. (Right) Relative capacity fade (normalized by the first cycle of a certain cell) before and after opening the cell, injecting additional volume of ordinary electrolyte and cell sealing by polyimide tape (no supercritical wash).

Although at first glance it seems that supercritical washing leads to sudden capacity drop after refilling, while simple cut immediately followed by electrolyte injection and resealing increases the capacity, we think that no conclusion can be drawn at this stage. The results are to be checked again with improved experimental conditions (control of the co-

solvent quality, external pressure applied to the cell after resealing). Even more accurate testing can be expected from experiments with HPEC (see the corresponding chapter of this report).
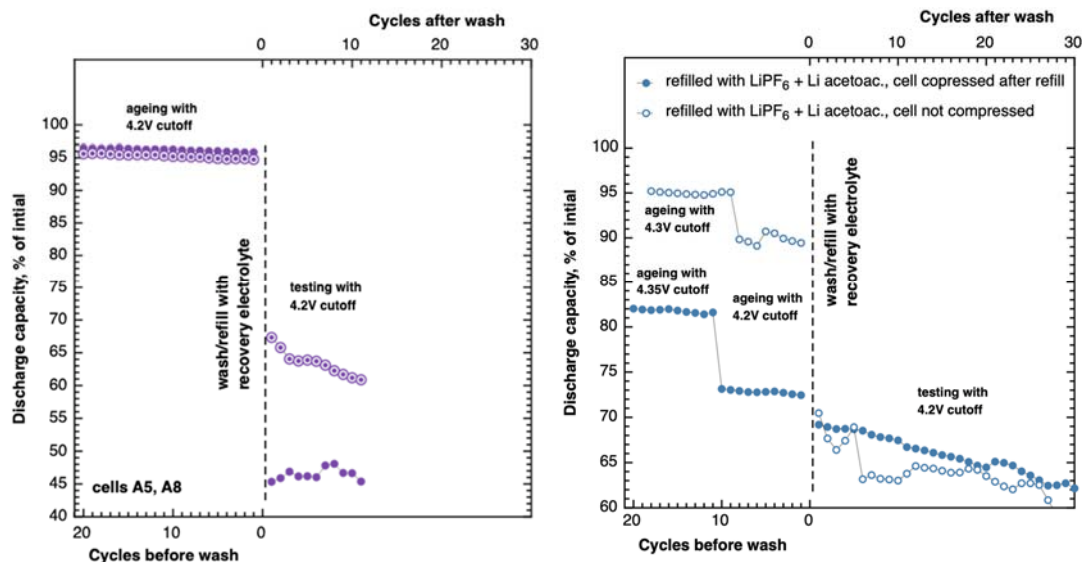

Figure 9. Relative capacity fade (normalized by the first cycle of a certain cell) before and after opening the cell, washing by SCF, refiling with recovery electrolyte candidate (nitrate-containing on the left, acetoacetate-containing on the right), and resealing by polyimide tape. The cells refilled with nitrate-containing electrolyte were cycled without external cell compression after refilling; acetoacetate-containing – with and without compression.

The aged cell refilling with few recovery electrolyte candidates, namely lithium nitrate, acetoacetate, and lactate, was further performed. As in the control experiments, we unfortunately got scattered data after cell refilling. Refilling with nitrate and acetoacetate showed no capacity improvement and, in major cases, acceleration of capacity degradation. Refilling with acetoacetate containing electrolyte was accompanied by refilled cell testing with and without applying external cell compression after refilling. Cycling the compressed cell after refilling showed lower capacity drop. The capacity fading, however, accelerated in both cases (compressed and non-compressed cells). Again, we note that these are just single observation requiring accurate reproducibility check.

Some promising results were unexpectedly obtained for lithium lactate-containing recovery electrolyte (lithium lactate showed nearly no oxidative currents in preliminary screening). Figure 10 demonstrates the results of refilling two pouch cells aged in a little bit different conditions, washed/refilled and further tested with and without the cell compression. Again, compressing the cell after refilling and sealing resulted in lower capacity drop. More important, the cells demonstrated capacity stabilization after refilling

in both experiments.

The obtained data do not evidence for capacity improvement after washing/refilling the pouch cells. Nevertheless, comparing the behavior of the lactate-containing electrolyte refilling with others and considering the unfavorable experimental conditions revealed by control experiments gives a hope that lactate-based recovery can help in battery performance recovery.
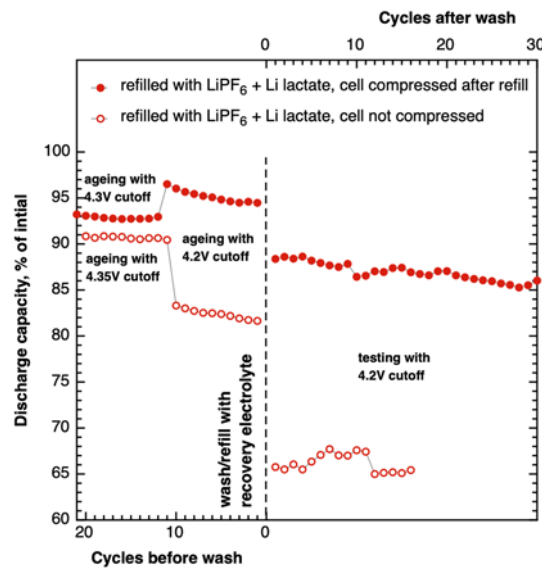

Figure 10 Relative capacity fade (normalized by the first cycle of a certain cell) before and after opening the cell, washing by SCF, refiling with lactate-containing recovery electrolyte, and resealing by polyimide tape.
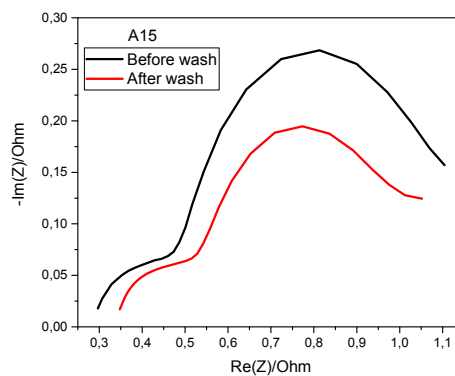

Figure 11 The EIS spectra of the pouch cell before and after washing/refilling with lactate-containing electrolyte. The cell was compressed after resealing.

Furthermore, comparison of the EIS spectra measured before and after the cell washing and refilling with a lactate-containing electrolyte (Figure 11) shows some decrease in the

diameter of the lower-frequency depressed semicircle, which can indirectly evidence for at least partial SEI removal. Additional EIS studies in more accurate conditions, as well as the cell C-rate testing before and after refilling are needed to clarify the possibility of battery power recovery.

High-pressure electrochemical cell design and testing

HPEC design

On the present stage of the project the concept and the design of high-pressure electrochemical cell has been developed. The purpose of HPEC development is performing electrochemical measurements and supercritical extraction experiments without disturbing the separator and the electrodes. Indeed, washing of pouch cells inevitably requires cutting off the pouch, which can affect the contact between the electrodes and separator, and might deteriorate the battery capacity. The capacity decrease depends randomly on how accurately this cutting off is performed. This causes significant random error in the experiment and requires multiple repetition of identical experiments to gather the reliable statistical data. This problem is solved in HPEC since it allows one to perform supercritical extraction and electrochemical measurements without touching the separator-electrode assembly.

HPEC consists of two main parts: inner 3-electrode electrochemical cell made of PEEK and outer high-pressure cell made of stainless steel (AISI 321) (Figure 12). Inner cell ensures reliable contact between the current collector and electrodes and separator. The outer cell can withstand high-pressure during supercritical extraction procedure and contains 5 high-pressure ports: 3 for the electrodes and 2 for supercritical fluid supply.

HPEC assembly scheme is presented in Figure 13. The PEEK inner cell consists of two parts: the upper part with a spike and the lower part with a slot for the spike (Figure 14). Both parts have internal threaded center holes for the electrodes. The lower part also has an off-center hole with a female thread for the reference electrode. The two parts are clamped using three M1.6 cylindrical head screws.
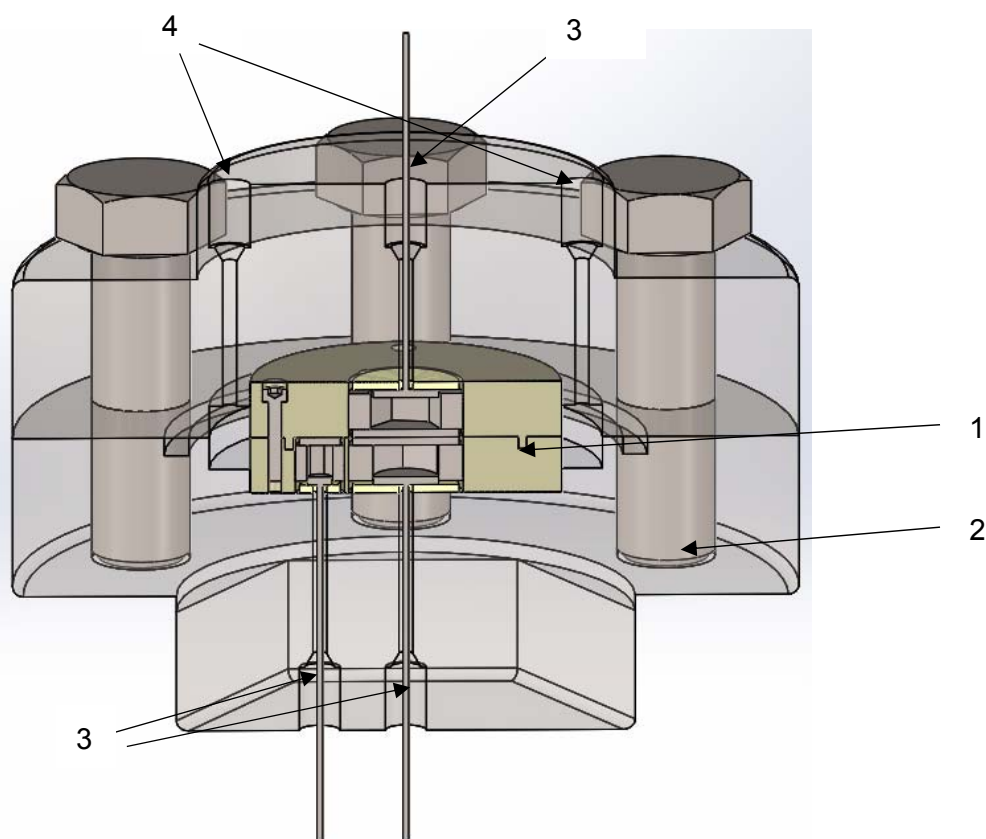
Figure 12. HPEC assembly. 1 – inner 3-electrode cell body made of PEEK. 2 – outer high pressure cell body made of stainless steel. 3 – high-pressure electrode ports. 4 – high-pressure gas ports.

First, inner cell is assembled. The separator is placed on the upper part of inner cell, the spike ensures centrals positioning of the separator. Then the lower part is attached and clamped with M1.6 cylindrical head screws. After that one electrode is placed on the separator, covered with electrode current-collector plate and fixed with electrode-holding nut. Then the inner cell is turned over, the second electrode and the reference electrode are placed on the separator, covered with the corresponding contact plates, and then fixed with the electrode-holding nuts. The assembled inner cell (Figure 15) is placed in the outer cell body.

Outer cell has a channel at the bottom of the housing for an O-ring rubber sealant. The two parts of the outer cell are pressed together with M12 hex bolts. In order to exclude the rotation of the PEEK cell inside the body and to ensure the position of the reference electrode is fixed, the PEEK cell has the shape of a circle with a cut-out segment, and the stainless-steel body has a correspondingly shaped recess.

The assembled PEEK inner cell has 8 rectangular channels (1.5×1 mm^2) for better supercritical fluid access to the electrodes.
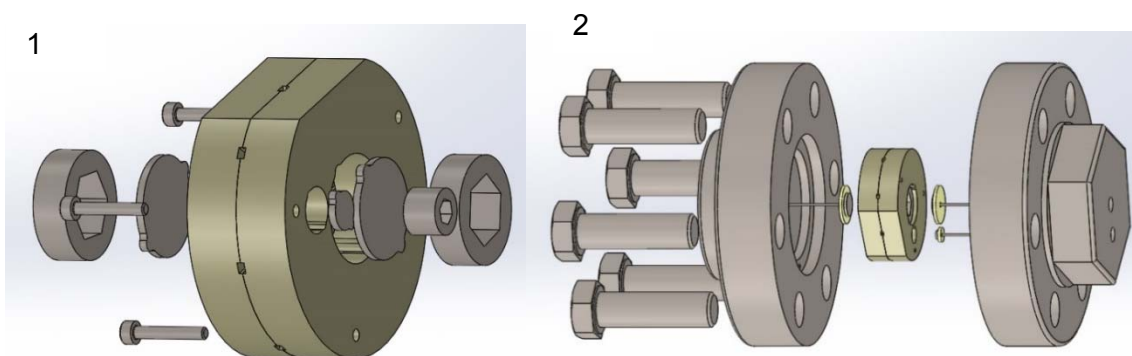
Figure 13. HPEC assembly scheme. 1 – inner electrochemical cell assembly. 2 – assembly of outer high-pressure cell with enclosed inner cell.
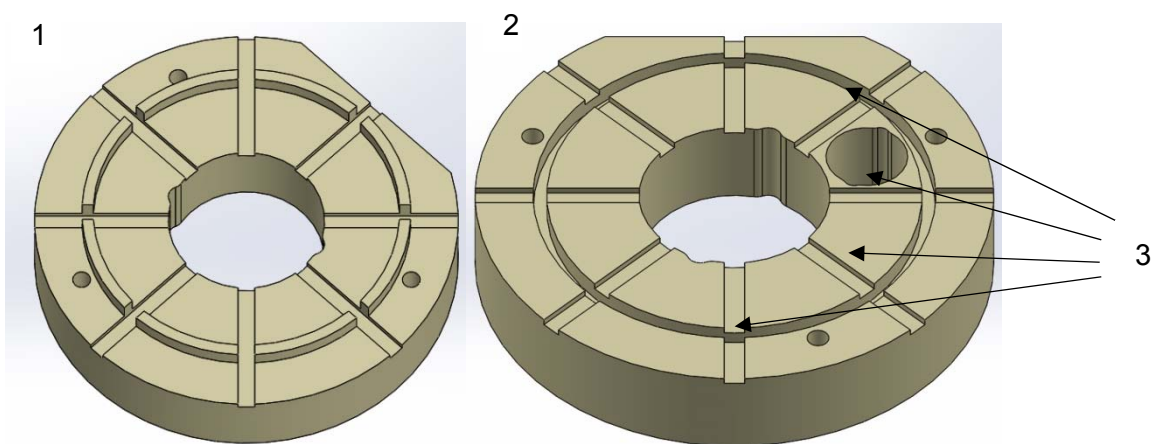

Figure 14. Inner cell body parts. 1 – upper part. 2 – lower part. 3 – 8 channels for supercritical fluid access to the electrodes and separator
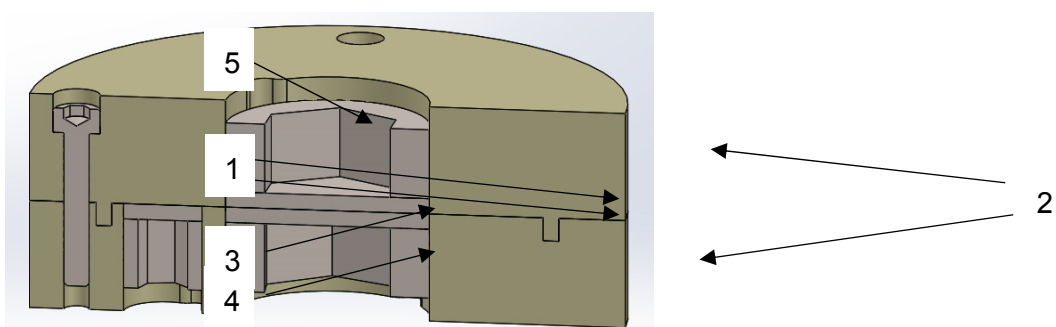

Figure 15. Inner 3-electrode electrochemical cell scheme. 1 – electrode current collector plates. 2 – electrode holding nuts. 3 – reference electrode contact plate. 4 – reference electrode holding nut. 5 – M1.6 inner cell holding screw (3 pcs.).

The electrical contact of the electrodes of the inner cell and the outer wire is provided by

means of metal springs placed inside the hexagonal cut of the nuts inside the PEEK cell (not shown in the figures).

The pictures of the fabricated HPEC are shown in Figure 16. The technical drawings of the HPEC parts are attached to the present report as an Appendix.


Figure 16 The photographs of HPEC

HPEC testing

To investigate the pressure resistance of the stainless-steel case, a computer simulation using SolidWorks software package was carried out. Figure 17 shows the distribution of stresses arising in the upper and lower parts of the body at an internal pressure of 600 bar. The modelling shows that the cell can withstand pressure of 600 bar without noticeable deformation. In a real experiment, the cell was successfully tested under the working pressure of 300 atm without any signs of gas release.
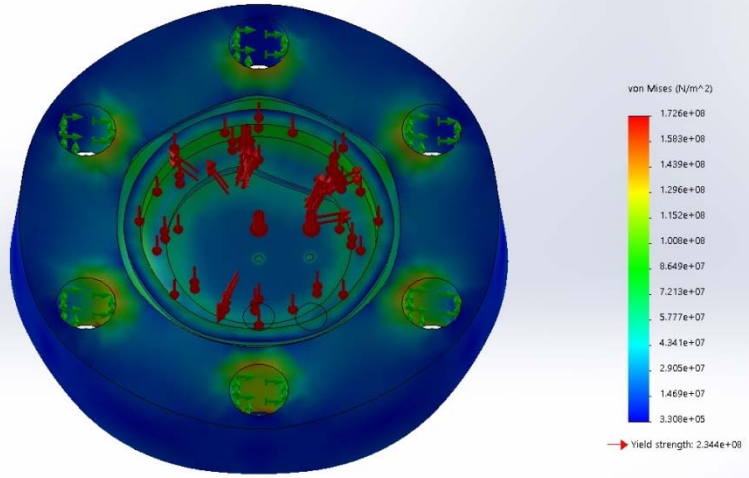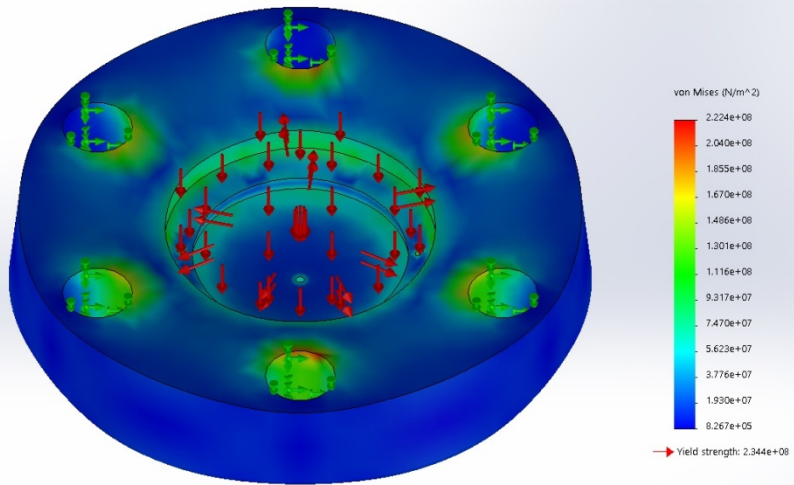
Figure 17. HPEC outer cell mechanical pressure resistance simulation results. Red arrows - pressure on this wall, green arrows - these sides are fixed with bolts.

To further check the electric contacts between the electrode terminals, contact springs and current collecting plates the impedance of the assembled HPEC cell without any electrodes and separator was measured (Figure 18). The contact impedance magnitude appears to be lower than 3 Ohm in the frequency range from 10 kHz to 10 mHz. Such contact resistance is low enough for Li-ion battery cycling inside HPEC.
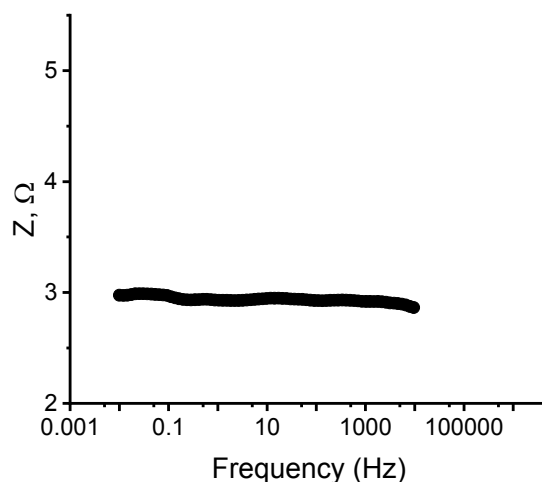
Figure 18. HPEC contact impedance.

For the electrochemical testing HPEC was assembled in two-electrode configuration. NMC811- and graphite-based electrodes were prepared in-house by Dr.Blade single-side coating the corresponding slurries onto aluminum and copper foils. Polypropylene single-layer separator soaked 1M LiPF$_6$ in EC:DMC was placed between the electrodes.

First HPEC runs revealed a problem of current-collector corrosion after ca. 20 h of cycling in standard CC-CV mode, which is depicted in Figure 19. After 6-8 cycles voltage hold resulted in the electrochemical noise on current transients. Visual examination of the cell showed corrosion of current collecting terminals (plates) and holding nuts, mainly on contacting faces. To avoid corrosion, we decreased amount of electrolyte, and added insulating spacers between holding nut and current collector.
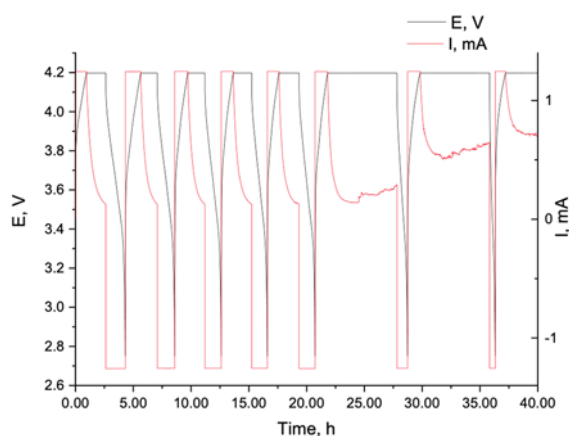

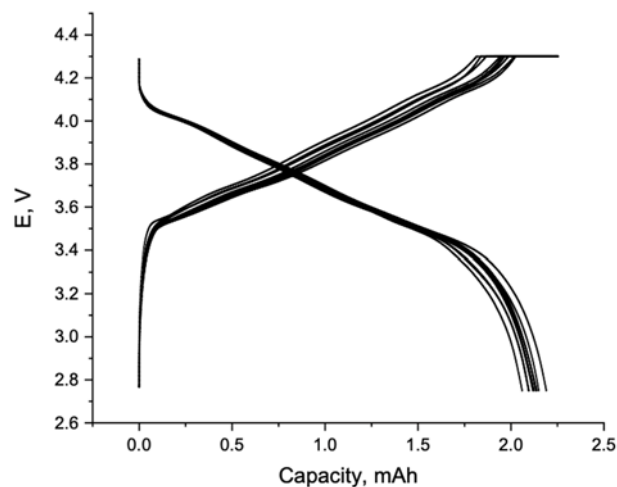*Figure 19 CC-CV testing of HPEC cell, NMC vs. graphite electrodes.*

Figure 20 Discharge/recharge voltage profiles for HPEC assembled with NMC vs. graphite electrodes.

New corrosion resistant current terminals were ordered, while temporary solution based on limited electrolyte volume and additional insulation allowed to perform the cycling inside the cell as shown in Figure 20. Unfortunately, using small electrolyte volume at the moment limits the measurements in three-electrode configuration due to the high RE impedance. This problem, however, will be tackled with charge to corrosion-resistant current collectors and increased electrolyte volume.
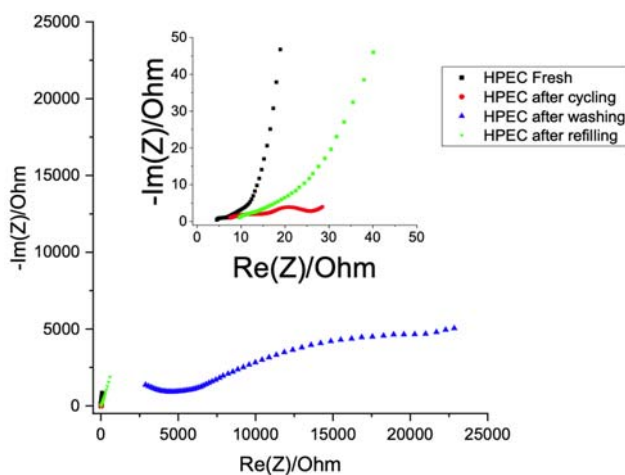

Figure 21 Electrochemical impedance spectra of the HPEC assembled with NMC vs. graphite electrodes after assembly, after 15 cycles, after washing and after refilling with an ordinary electrolyte. The inset demonstrates low-impedance region of the plot.

Further, washing and the electrolyte refilling ability were checked with HPEC. Figure 21 shows the EIS data for HPEC right after the assembly, after 15 cycles, after the cell

washing with SCF, and, finally, after refilling with an ordinary electrolyte. The cell internal impedance increases after cycling. The cell washing with SCF results in the impedance rise by few orders of magnitude due to the flushing of the electrolyte out from the cell. Refilling the cell again leads to normalization of the cell resistance evidencing filling of the electrodes and separator with electrolyte.

Concept of the rig for LIB recovery

The conceptual idea of the system (or rig) for LIB recovery is shown in Figure 22. The elaboration of this idea becomes reasonable if the suggested approach – washing of the cells and refilling them with a specially developed electrolytes for recovery – will be demonstrated efficient for restoring the battery capacity and/or power. The criteria of recovery efficiency are not clear now; it is obvious, however, that such criteria should consider not only the technical parameters but also the economic estimates helping to compare the battery second-life performance improvement idea with LIB recycling.
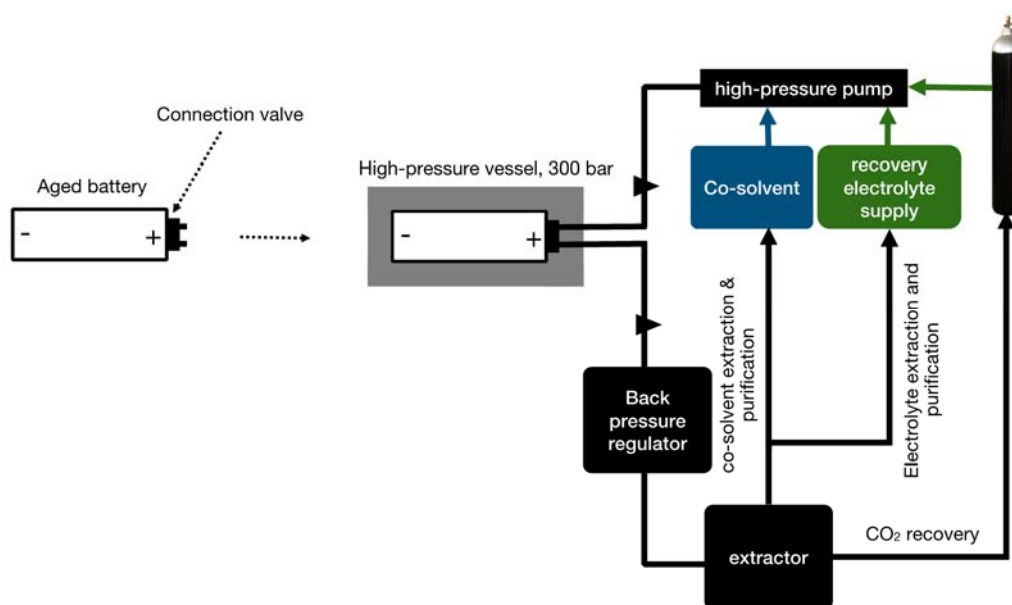

Figure 22 The concept of possible future system (rig) for LIB washing and refiliing.

General idea can be described already. Indeed, the details are dependent on the cell type (pouch, prismatic, cylindrical) used in EV battery pack. If the cells with hard case are used, it should have a special integrated valve for the connection to the recovery station. For pouch cells the connection can be established without any valve by means of two needles making two small holes in the pouch body. The industrial-scale resealing approach is to be developed and tested separately.

The battery cell itself has a light enclosure, which cannot withstand high pressure. So, the recovery station shall provide a high pressure-safe reactor, in which the cells are punched (for pouch cells) or connected to high-pressure supply via an integrated valve.

Old electrolyte extraction by SCF and cell refilling are to be done sequentially. Components of the SCF are captured and used in a closed cycle. The extracted electrolyte can be purified for future use or for recovery electrolyte preparation in a separate cycle. Thus, the electrolyte consumption can be minimized.

As the cells require formation cycle after recovery, the recovery station shall have an electric connection to the cell to perform the formation before taking the cell out of the pressure-tight system to the environment.

Conclusions

- Manual opening/"resealing" (by adhesive tape) of the pouch cells lead to sufficient inaccuracy. Hard to check the effect of washing/recovery electrolyte refilling.
- "Resealed" pouch cells tend to degrade faster; however, refilling it with Li lactate-containg recovery electrolyte significantly slows down the degradation. It gives a hope that capacity will raise if experimental conditions are improved. It should be checked in HPEC enabling more accurate experiments.
- Project timeframe is not enough for proper ageing of good-quality pouch cells. Overcharging the cells to speed up the project can lead to unpredictable results. We need either more time, or employing express ageing techniques based on elevated temperature.
- HPEC was fabricated and tested. It is operational, nevertheless, further improvements in design are needed. Checking the obtained results in HPEC is already possible and ongoing.

Challenges for the future

- Establishing reproducible cell ageing protocol within reasonable timeframe.
- Further improvement of HPEC design and testing: extending corrosion resistance, decreasing internal volume, testing with the reference electrode. Fabricating more cells for speeding up the experiments.
- Thorough checking all the recovery electrolyte candidate in HPEC. Reproduction of the results for the aged pouch cells using the most successful candidates.

References

1. Sharma S.S., Manthiram A. Towards more environmentally and socially responsible batteries // Energ Environ Sci. 2020. Vol. 13, № 11. P. 4087–4097.

2. Xu J. et al. A review of processes and technologies for the recycling of lithium-ion secondary batteries // J Power Sources. 2008. Vol. 177, № 2. P. 512–527.

3. Zeng X., Li J., Singh N. Recycling of Spent Lithium-Ion Battery: A Critical Review // Crit Rev Env Sci Tec. 2014. Vol. 44, № 10. P. 1129–1165.

4. Ordoñez J., Gago E.J., Girard A. Processes and technologies for the recycling and recovery of spent lithium-ion batteries // Renewable and Sustainable Energy Reviews. 2016. Vol. 60, № C. P. 195–205.

5. Zheng X. et al. A Mini-Review on Metal Recycling from Spent Lithium Ion Batteries // Engineering. 2018. Vol. 4, № 3. P. 361–370.

6. Gaines L. The future of automotive lithium-ion battery recycling: Charting a sustainable course // SUSMAT. 2014. Vol. 1–2, № C. P. 2–7.

7. Martinez-Laserna E. et al. Battery second life: Hype, hope or reality? A critical review of the state of the art // Renew Sustain Energy Rev. 2018. Vol. 93. P. 701–718.

8. Birkl C.R. et al. Degradation diagnostics for lithium ion cells // Journal of Power Sources. 2017. Vol. 341, № C. P. 373–386.

9. Rumberg B. et al. Identification of Li ion battery cell aging mechanisms by half-cell and full-cell open-circuit-voltage characteristic analysis // Journal of Energy Storage. 2019. Vol. 25. P. 100890.

10. Elliott M. et al. Degradation of electric vehicle lithium-ion batteries in electricity grid services // J Energy Storage. 2020. Vol. 32. P. 101873.